


Influence of large-scale teleconnections on annual and seasonal floods in Godavari and Narmada River basins

Sunil Gurrapu ^{a,*}, Ashwini Ranade^{a,b} and Jagadish Prasad Patra^b

^a Water Resources Systems Division, National Institute of Hydrology, Roorkee, India

^b Surface Water Hydrology Division, National Institute of Hydrology, Roorkee, India

*Corresponding author. E-mail: gurrapus@gmail.com

 SG, 0000-0002-0996-1276

ABSTRACT

Indian summer monsoon rainfall is strongly influenced by large-scale atmosphere-ocean oscillations including Pacific Decadal Oscillation (PDO), El Niño-Southern Oscillation (ENSO), and Indian Ocean Dipole (IOD). Researchers have shown that the negative phase of PDO or La Niña episodes of ENSO produce higher magnitude rainfall and hence relatively wetter years. So, it is imperative to have better knowledge of flood characteristics in the Indian watersheds for optimal planning and design of various infrastructure, and for optimal planning and management of reservoir operations. Traditionally, such information is estimated using flood frequency analysis (FFA), however the adequacy of traditionally accepted assumption that the annual peak flows are independent and identically distributed (i.i.d.) is questioned globally. This study evaluates the adequacy of this assumption in Godavari and Narmada River basins and assesses the influence of PDO, ENSO and IOD on flood characteristics. The results indicate that the flood characteristics at the majority of gauges are significantly influenced by these oscillations, higher magnitude floods are associated with negative episodes. A very few gauges are inversely related to these teleconnections, although statistically not significant. Overall, the signal of all the three teleconnections is found in the annual and seasonal floods in the majority of gauging stations.

Key words: El Niño-Southern Oscillation, flood frequency, Indian Ocean Dipole, non-stationarity, Pacific Decadal Oscillation, quantile-quantile plots

HIGHLIGHTS

- Annual and seasonal peak flows in selected gauges indicate that flood characteristics are substantially influenced by PDO, ENSO or IOD.
- Higher magnitude floods are more common during the negative phase of PDO or during the La Niña episode.
- The results highlight the potential inadequacy of the i.i.d. assumption.
- The knowledge of regional hydroclimate with regard to large-scale atmosphere-ocean oscillations should be considered.

INTRODUCTION

In India, flooding is one of the three prominent climate extremes, the other two being droughts and cyclones (Bhattacharya & Das 2007). The majority of flooding in Indian watersheds occurs during summer monsoon months due to uneven distribution of rainfall. For example, the recent devastating floods in Kerala were in response to the abnormally high rainfall received within a short period of 3 days, i.e. from 15th to 17th August 2018 (e.g. Mishra *et al.* 2018). Approximately 80% of rainfall over the Indian subcontinent is received during the summer monsoon. Summer monsoon rainfall being the major source of water input to the Indian subcontinent, optimal design and operation of water resources infrastructure (e.g. major dams) is very much essential.

The Indian summer monsoon is substantially influenced by several low-frequency atmosphere-ocean oscillations including Pacific Decadal Oscillation (PDO), El Niño-Southern Oscillation (ENSO), Indian Ocean Dipole (IOD), Atlantic Multidecadal Oscillation (AMO), etc. (e.g. Walker 1933; Saji *et al.* 1999; Roy *et al.* 2003; Sajani *et al.* 2007; Krishnamurthy & Krishnamurthy 2013a, 2013b; Li *et al.* 2017; Saini *et al.* 2022). For example, Krishnamurthy & Krishnamurthy (2013a) identified that the warm phase of PDO is associated with the rainfall deficit over the Indian subcontinent, whereas the cool phase

This is an Open Access article distributed under the terms of the Creative Commons Attribution Licence (CC BY 4.0), which permits copying, adaptation and redistribution, provided the original work is properly cited (<http://creativecommons.org/licenses/by/4.0/>).

of PDO is associated with the rainfall excess. A similar relationship is identified between El Niño and La Niña episodes of ENSO pattern (e.g. Krishnamurthy & Krishnamurthy 2013a; Saini *et al.* 2022). Despite these studies on teleconnections and Indian summer monsoon rainfall (ISMR), there has been little work done on the influence of these teleconnections on annual mean and/or peak streamflow in the watersheds of the Indian subcontinent. Henceforth, this study explores the influence of such teleconnections, i.e. PDO, ENSO and IOD specifically, on the characteristics of annual floods (or annual peak flows) in the Godavari and Narmada River basins. Such information plays an important role in the optimal planning and design of various infrastructures, and informs adaptive management policy for better reservoir operations.

The existing knowledge of flood characteristics in the Indian watersheds is primarily based on the assumption of stationarity, i.e. the annual floods are independent and identically distributed (*i.i.d.*) or the system fluctuates within a fixed envelope of variability (e.g. Milly *et al.* 2008). However, this assumption is widely questioned across the globe and several studies indicate that this assumption is inadequate (e.g. Milly *et al.* 2008; Stedinger & Griffis 2008; Gurrapu *et al.* 2016; 2022). For example, Franks (2002) and Kiem *et al.* (2003) demonstrated that the frequency of floods in New South Wales, Australia is impacted by Inter-Decadal Pacific Oscillation (IPO) and ENSO. They suggest that annual peak flow data should be assessed as a function of the causal climatological factors that affect regional climates. In a similar study, Ward *et al.* (2014) determined that La Niña episodes produce higher annual floods compared with El Niño episodes in the majority of the river basins across the globe, whereas few basins show the opposite relation. In another study, Andrews *et al.* (2004) determine that El Niño episodes produced higher annual floods along the California coast, USA. In a more recent study, Gurrapu *et al.* (2016) demonstrated that the frequency of floods in the watersheds of western Canada is substantially impacted by a large-scale low-frequency PDO, where the negative phase of PDO produced higher magnitude floods and the positive phase of PDO produced relatively lesser magnitude floods. So, the existing know-how on the flood characteristics of the Indian watersheds becomes immaterial unless proven. Therefore, this study explores the relationships between annual floods in the selected watersheds and the large-scale low-frequency atmospheric oscillations including ENSO, PDO and IOD.

This study is motivated by the observation that such teleconnections are not yet a key ingredient in the planning and design of regional water resources and/or transportation infrastructure. This study is the first of its kind to evaluate the impact of these low frequency oscillations, which are known to substantially control the magnitude and frequency of ISMR, on the annual and seasonal, i.e. summer monsoon (southwest or SW) and winter (northeast or NE) monsoon peak flows in Godavari and Narmada River basins.

STUDY AREA AND DATA

To evaluate the influence of the PDO, ENSO and IOD on annual or seasonal maximum daily streamflows, recorded daily streamflow data from 64 streamflow gauging stations (Figure 1 and Table 1) spread across Godavari (46 gauges) and Narmada (18 gauges) River basins were chosen. The Godavari River basin is an east flowing river draining into the Bay of Bengal and is spread across the states of Maharashtra, Madhya Pradesh, Chhattisgarh, Odisha, Andhra Pradesh, Telangana and Karnataka, whereas the Narmada River Basin is a west flowing river draining into the Arabian Sea and is spread across the states of Madhya Pradesh and Gujarat. All the selected gauging sites are operated and maintained by Central Water Commission (CWC) and the observed daily streamflow data is available from India-WRIS (India Water Resources Information Systems; <https://indiawris.gov.in/wris/#/DataDownload>) website for free. The selected gauging stations were chosen based on the available length of daily streamflow data, i.e. each station has at least 15 years of streamflow data, whether continuous or discontinuous. The gross drainage area of the selected sub-basins ranges between 787 and 3,07,800 km².

Annual peak flow in Godavari and Narmada Rivers typically occurs during the southwest (i.e. during June–September) and/or northeast (i.e. during October–December) monsoon seasons, from the high magnitude and/or high intensity rainfall. The time series of annual peak flows, the maximum of the daily streamflow recorded during a water year starting from 1st June and ending on 31st May of the following year, at each station are extracted from the daily averaged streamflow records. In addition, the time series of seasonal peak flows, i.e. from 1st June to 30th September for SW monsoon and from 1st October to 31st December for NW monsoon, are extracted for each station. At each gauging site, peak flows for any given year or season are extracted from all the available data, regardless of the missing data. Any year or season with missing daily streamflow data or with a '0' mean streamflow is discarded and is not used in the analysis. Details of the selected streamflow gauging

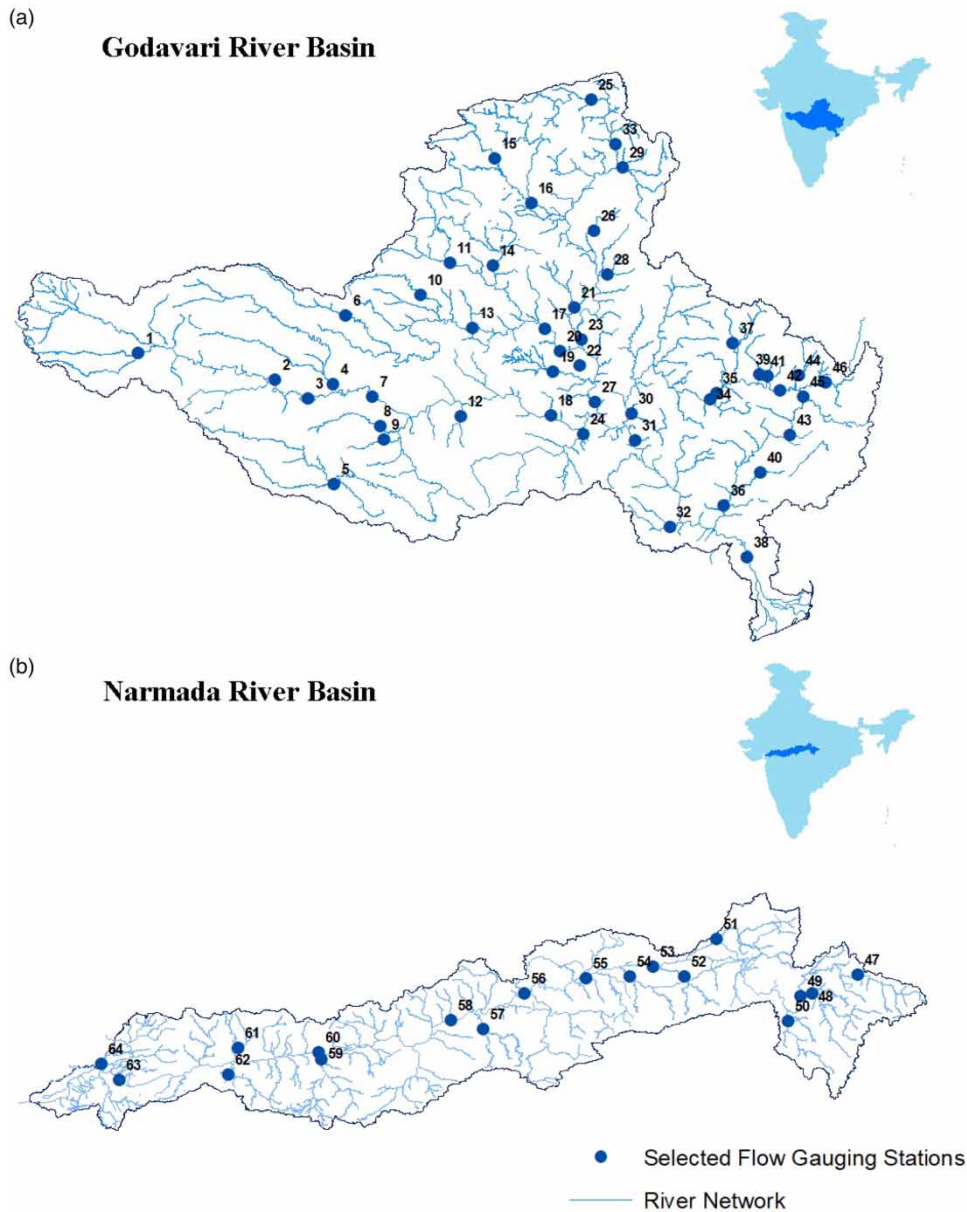


Figure 1 | Locations of all the selected streamflow gauging stations from (a) Godavari and (b) Narmada River basins. The numbers given are associated with the ID column of Table 1, which provide the details of each gauging station.

stations and the recorded daily streamflow data for all the selected gauging stations are downloaded freely from the India-WRIS website (<https://indiawris.gov.in/wris/#/DataDownload>).

The magnitude of PDO is quantified by several institutes from across the world and in this study, PDO indices from the Joint Institute for the Study of Atmosphere and Ocean (JISAO), University of Washington (<http://jisao.washington.edu/pdo/>) (Mantua *et al.* 1997), were used. To analyze the influence of PDO on annual peak flows, June–December (summer and winter monsoon seasons together) monthly averaged PDO index ($\text{PDO}_{\text{Jun_Dec}}$) was used. Similarly, to analyze the influence of PDO on seasonal peak flows, June to September monthly averaged PDO index (PDO_{JJAS}) for SW monsoon and October to December monthly averaged PDO index (PDO_{OND}) were used. The temporal variability of $\text{PDO}_{\text{Jun_Dec}}$ and the JISAO defined phases of PDO can be seen in Figure 2. In this study, the influence of PDO on annual and/or seasonal peak flows was analyzed based on the magnitude of the PDO index, by categorizing them into positive (threshold value = 0.5) and negative (threshold value = -0.5) episodes of PDO. To do so, for example, the annual peak flow series at each station

Table 1 | List of the 64 selected streamflow gauges in Godavari and Narmada basins from the IWRIS database, with their station codes, names, location and other important particulars

ID	IWRIS ID	Stn ID	Station name	Latitude	Longitude	Catchment area	Tributary name	Basin name	Start year	End year	Gauge type
1	AGU00D3	GPAC02	Pachegaon	19.53	74.83	5,800	Pravara	Godavari	1979	2015	Regulated
2	AG00059	GDHA03	Dhalegaon	19.23	76.36	30,840	Godavari	Godavari	1965	2015	Regulated
3	AG000R6	GGRB04	G.R. Bridge	19.02	76.73	33,934	Godavari	Godavari	1976	2015	Regulated
4	AGR00A5	GPUR05	Purna	19.18	77.01	15,000	Purna	Godavari	1968	2015	Regulated
5	AGP00N8	GSAI06	Saigaon	18.06	77.02	9,960	Manjira	Godavari	1965	2015	Regulated
6	AGH32R8	GKAN07	Kanergaon	19.96	77.15	3,515	Pranhitha	Godavari	1991	2017	Natural
7	AG000P3	GYEL09	Yelli	19.04	77.45	53,630	Godavari	Godavari	1976	2015	Regulated
8	AGP10F7	GBET10	Betmogra	18.71	77.54	2,105	Manjira	Godavari	1997	2015	Natural
9	AGP20F4	GDEG11	Degloor	18.56	77.58	1,900	Manjira	Godavari	1984	2015	Regulated
10	AGH35G0	GMAN12	Mangrul	20.19	77.99	2,500	Pranhitha	Godavari	1992	2017	Natural
11	AGH30Q1	GHIV13	Hivra	20.55	78.32	10,240	Pranhitha	Godavari	1987	2017	Regulated
12	AGM00G6	GGAN14	Gandlapet	18.8	78.44	1,360	Peddavagu	Godavari	1986	2015	Natural
13	AGH32D5	GPGB15	P.G. (Penganga) Bridge	19.82	78.57	18,441	Pranhitha	Godavari	1965	2017	Regulated
14	AGH3AF4	GNAN16	Nandgaon	20.52	78.8	4,580	Pranhitha	Godavari	1986	2017	Regulated
15	AGH4BQ3	GRAM17	Ramakona	21.72	78.82	2,500	Pranhitha	Godavari	1986	2017	Natural
16	AGH4BF6	GSAT18	Satrapur	21.22	79.23	11,100	Pranhitha	Godavari	1984	2017	Regulated
17	AGH30E2	GBAM19	Bamini (Balharsha)	19.81	79.38	46,020	Pranhitha	Godavari	1965	2017	Regulated
18	AG000J3	GMAN20	Mancherial	18.83	79.45	102,900	Godavari	Godavari	1965	2015	Regulated
19	AGH10L0	GBHA21	Bhatpalli	19.32	79.47	3,100	Pranhitha	Godavari	1986	2017	Regulated
20	AGH30B6	GSIR22	Sirpur	19.55	79.55	47,500	Pranhitha	Godavari	1965	2015	Regulated
21	AGHA1Q4	GRAJ23	Rajoli	20.05	79.71	1,900	Pranhitha	Godavari	1986	2017	Natural
22	AGR10C6	GZAR24	Zari	19.39	79.77	5,550	Purna	Godavari	1986	2015	Natural
23	AGH40A4	GASH25	Ashti	19.68	79.79	50,990	Pranhitha	Godavari	1965	2017	Regulated
24	AGI00C3	GSOM26	Somanpally	18.62	79.81	12,691	Maner	Godavari	1964	2014	Regulated
25	AGH40V3	GKEO27	Keolari	22.38	79.9	2,970	Pranhitha	Godavari	1986	2017	Regulated
26	AGH49I1	GSAL28	Salebardi	20.91	79.93	1,800	Pranhitha	Godavari	1985	2017	Natural
27	AGH00C4	GTEK29	Tekra	18.98	79.94	108,780	Pranhitha	Godavari	1964	2017	Regulated
28	AGH46D4	GWAI30	Wairagarh	20.42	80.08	2,600	Pranhitha	Godavari	1992	2017	Natural
29	AGH4MC3	GRAJ31	Rajegaon	21.62	80.25	5,380	Pranhitha	Godavari	1985	2017	Regulated
30	AGG00B5	GPAT32	Pathagudem	18.85	80.35	40,000	Indravathi	Godavari	1965	2015	Regulated
31	AG000G7	GPER33	Perur	18.55	80.39	268,200	Godavari	Godavari	1965	2015	Regulated

(Continued.)

Table 1 | Continued

ID	IWRIS ID	Stn ID	Station name	Latitude	Longitude	Catchment area	Tributary name	Basin name	Start year	End year	Gauge type
32	SANGAM	GSAN35	Sangam	17.58	80.78	1,565	Murredu	Godavari	1996	2014	Natural
33	AGH40R6	GKUM37	Kumhari	21.88	81.17	8,070	Pranhitha	Godavari	1986	2017	Regulated
34	AGG60B1	GTUM38	Tumnar	19.01	81.23	1,700	Indravathi	Godavari	1989	2015	Natural
35	AGG00N7	GCHI39	Chindnar	19.08	81.3	17,270	Indravathi	Godavari	1971	2015	Regulated
36	AGC00C5	GKON40	Konta	17.82	81.39	19,550	Sabari	Godavari	1964	2015	Regulated
37	CHERRIBEDA	GCHE41	Cherribeda	19.64	81.49	890	Indravathi	Godavari	1996	2014	Natural
38	AG000C3	GPOL43	Polavaram	17.24	81.65	307,800	Godavari	Godavari	1965	2015	Regulated
39	AGC90C8	GAMB45	Ambabal	19.29	81.79	1,968	Indravathi	Godavari	1989	2015	Natural
40	AGC20H2	GPOT46	Potteru	18.19	81.8	1,120	Sabari	Godavari	1989	2015	Regulated
41	AGG91F2	GSON47	Sonarpal	19.27	81.88	1,523	Markandi	Godavari	1989	2015	Natural
42	AGG00R9	GJAG48	Jagdapur	19.11	82.02	7,380	Indravathi	Godavari	1964	2015	Regulated
43	AGC00N4	GSAR49	Saradaput	18.61	82.13	3,047	Sabari	Godavari	1968	2015	Regulated
44	KOSAGUMDA	GKOS50	Kosagumda	19.28	82.23	1,635	Indravathi	Godavari	1996	2014	Natural
45	AGC40E9	GMUR51	Murthahandi	19.04	82.28		Indravathi	Godavari	1979	2015	Regulated
46	AGG00U7	GNOW52	Nowrangpur	19.2	82.53	3,445	Indravathi	Godavari	1965	2015	Regulated
47	10215001	NDIN01	Dindori	22.95	81.08	2,292	Narmada	Narmada	1988	2016	Regulated
48	10215004	NMOH02	Mohgaon	22.76	80.62	3,919	Burhner	Narmada	1977	2016	Regulated
49	10215002	NMAN03	Manot	22.74	80.51	4,667	Narmada	Narmada	1976	2016	Regulated
50	NCA SITE	NBAM04	Bamni Banjar	22.48	80.38	1,864	Banjar	Narmada	1972	2016	Natural
51	10215009	NPAT05	Patan	23.31	79.66	3,950	Heran	Narmada	1979	2016	Regulated
52	10215010	NBEL06	Belkheri	22.93	79.34	1,508	Sher	Narmada	1977	2016	Natural
53	10215011	NBAR07	Barman at Narmada (Barmanghat)	23.03	79.02	26,453	Narmada	Narmada	1971	2016	Regulated
54	10215012	NGAD08	Gadarwara	22.93	78.79	2,270	Shakkar	Narmada	1977	2016	Natural
55	10215013	NSAN09	Sandia	22.92	78.35	33,953	Narmada	Narmada	1978	2016	Regulated
56	10215019	NHOS10	Hoshangabad	22.76	77.73	44,548	Narmada	Narmada	1972	2016	Regulated
57	10215020	NCHH11	Chhidgaon	22.4	77.31	1,729	Ganjal	Narmada	1976	2016	Natural
58	10215022	NHAN12	Handia	22.49	76.99	54,027	Narmada	Narmada	1977	2016	Regulated
59	10215025	NKOG13	Kogaon	22.1	75.68	3,919	Kundi	Narmada	1972	2016	Regulated
60	1021615026	NMAN14	Mandleshwar	22.17	75.66	72,809	Narmada	Narmada	1971	2016	Regulated
61	NCA DHULSAR	NDHU15	Dhulsar	22021	74.85	787	Uri	Narmada	1999	2016	Natural
62	NCA PATI	NPAT16	Pati	21.94	74.75	2,151	Goi	Narmada	1999	2016	Natural
63	10215030	NGAR17	Garudeshwar	21.89	73.65	87,892	Narmada	Narmada	1972	2016	Regulated
64	10215032	NCHA18	Chandwada	22.05	73.47	3,846	Orsang	Narmada	1979	2015	Regulated

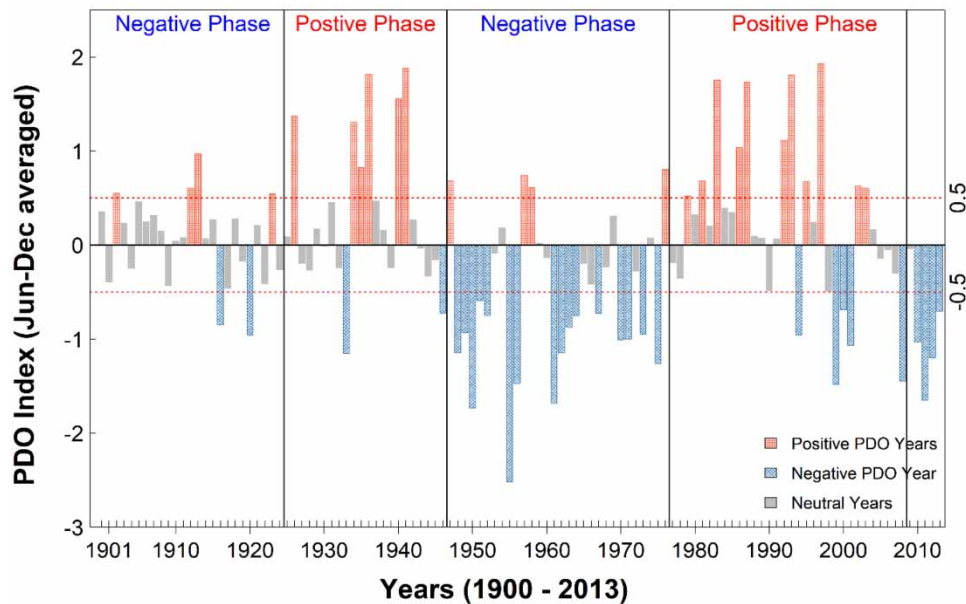


Figure 2 | Variability in the Pacific Decadal Oscillation (PDO) as represented by the June to December averaged PDO index ($\text{PDO}_{\text{Jun_Dec}}$) for the period 1900–2013, together with the thresholds (dotted lines), beyond which the PDO is considered to be strong.

are stratified as the basin's hydrological response to positive ($\text{PDO}_{\text{Jun_Dec}} \geq 0.5$) and negative ($\text{PDO}_{\text{Jun_Dec}} \leq -0.5$) episodes of the PDO (e.g. Gurrapu *et al.* 2016).

In order to directly compare the results from the low-frequency PDO to those from the higher-frequency ENSO, its influence on annual peak streamflow is also analyzed. ENSO is quantified in several ways by various institutes across the globe. In this study, the Oceanic Niño Index (ONI) is used to categorize the ENSO events (National Oceanic and Atmospheric Administration, NOAA, <https://psl.noaa.gov/data/correlation/oni.data>). In this study, June to December monthly averaged ENSO index ($\text{ONI}_{\text{Jun_Dec}}$) is used to evaluate the influence on annual peak flows, June to September monthly averaged index (ONI_{JJAS}) for SW monsoon, and October to December monthly averaged index (ONI_{OND}) for the NE monsoon seasonal peak flows. The temporal variability of $\text{ONI}_{\text{Jun_Dec}}$ over the past century can be seen in Figure 3. Using $\text{ONI}_{\text{Jun_Dec}}$, the annual peak flow series at each of the selected gauging stations are stratified as responses to El Niño ($\text{ONI}_{\text{Jun_Dec}} \geq 0.5$) and La Niña ($\text{ONI}_{\text{Jun_Dec}} \leq -0.5$) episodes of ENSO (Figure 3).

In addition to these two indices, the influence of the IOD is also evaluated. Sustained changes in the difference between sea surface temperatures of the tropical western and eastern Indian Ocean are known as IOD; more details of this oscillation are available at www.bom.gov.au/climate/iod/. IOD is quantified by Dipole Mode Index (DMI; Saji *et al.* 1999) and is freely available from Earth Systems Research Laboratory (ESRL), National Oceanic and Atmospheric Administration (NOAA), USA. DMI is computed at a monthly timescale and in this study, June to December monthly averaged index ($\text{DMI}_{\text{Jun_Dec}}$) is used for annual floods, June to September monthly averaged index (DMI_{JJAS}) for SW monsoon and October to December monthly averaged index (DMI_{OND}) for NE monsoon seasonal peak flows. Using $\text{DMI}_{\text{Jun_Dec}}$, the annual peak flow series at each of the selected gauging stations are stratified as responses to positive ($\text{DMI}_{\text{Jun_Dec}} \geq 0.5$) and negative ($\text{DMI}_{\text{Jun_Dec}} \leq -0.5$) episodes of IOD.

METHODS

The effect of large-scale teleconnections on maximum (annual and/or seasonal) flows in the Godavari and Narmada River basins is first analyzed by measuring the strength of correlation between them using non-parametric Spearman's correlation coefficient (ρ). Rank-based Spearman's correlation is a robust method with no prior assumption of a distribution-fit to the hydrological or meteorological data (Wilks 2006; Gurrapu *et al.* 2016). In this study, the correlation between the peak flows and each of the teleconnections, namely, PDO, ENSO (ONI) and IOD (DMI), at all the 64 gauging sites were computed and the correlation coefficient (Spearman's ρ) with p -value less than or equal to 0.1 is considered significant at a 90%

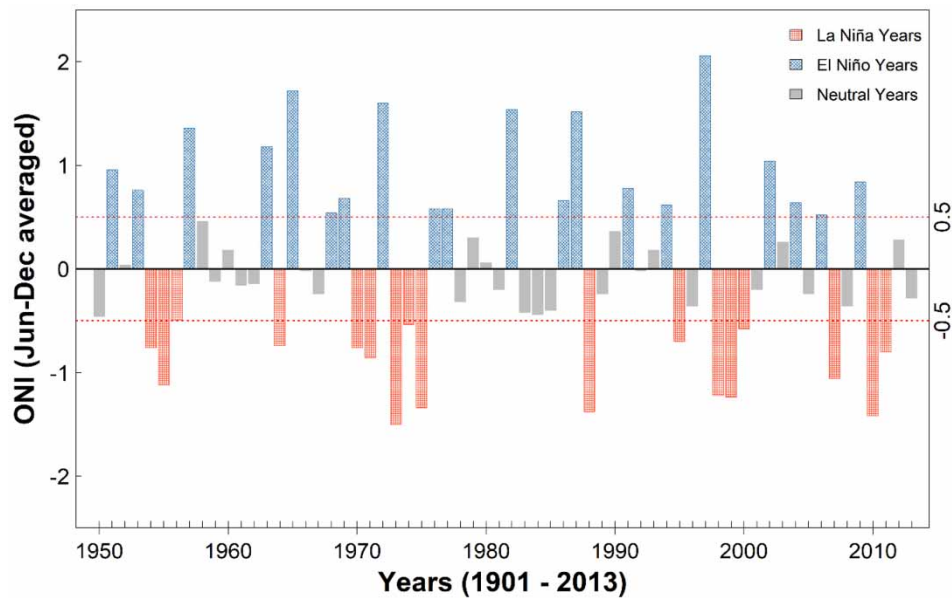


Figure 3 | Variability in the El Niño-Southern Oscillation (ENSO) as represented by the June to December monthly averaged Oceanic Niño Index (ONI_{Jun_Dec}) for the period 1950–2013, together with the lower and upper limits for categorizing into El Niño and La Niña episodes.

confidence level (i.e. based on the two-tailed significance test with $\alpha = 0.05$). The longest length of streamflow data enables the detection of the impact of teleconnections and so the full period of record was used in the analysis.

The effect of these teleconnections on the peak flows is further explored by stratifying the peak flow datasets according to the negative and positive episodes of PDO, ENSO and IOD and constructing quantile-quantile (Q-Q) plots. Q-Q plots are constructed based on the quantiles extracted from the stratified annual peak flow data (Helsel & Hirsch 2002; Gurrapu *et al.* 2016). The quantiles of the negative episodes (y -axis) are plotted against the quantiles of the positive episodes (x -axis) (i.e. for an individual point (x_i, y_i) of the plot, x_i is the peak flow of the i th ranked flood of the positive episode, and y_i is the peak flow of the i th ranked flood of the negative episode). The ratio of an i th ranked flood, i.e. $r_i = y_i/x_i$, from both episodes gives an indication of the impact of the chosen teleconnection. If this ratio is approximately equal to 1, it may be assumed that the i th ranked flood in both episodes is identical, however, it indicates otherwise if the ratio is greater or lesser than 1. If $r_i < 1$, it indicates that the i th ranked flood of the positive episode is higher than that of the negative episode and vice-versa. If the mean ratio R (Equation (1)) is approximately equal to 1 or if the points fall along the 1:1 line, the peak flow datasets may be assumed to be identically distributed or are sample datasets from the same population. In such a case, the peak flows at that gauging site are not affected by that specific teleconnection. The significance of the ratio, R was tested at $\alpha = 0.1$ significance level, i.e. 90% confidence level, using a two-sided permutation test with 10,000 iterations (Manly 2007; Gurrapu *et al.* 2016).

$$R = \sum_{i=1}^n \frac{y_i}{x_i} \quad (1)$$

Flood frequency curves fitted to the stratified peak flows help in investigating the impact of the teleconnections (e.g. Gurrapu *et al.* 2016). In this study, stratified peak flows were fit to a 3-parameter lognormal distribution (LN3) and 90% confidence intervals were constructed (USGS 1982). A clear separation between the flood frequency curves and non-overlapping confidence intervals indicate that the peak flows are not identically distributed (e.g. Franks & Kuczera 2002; Gurrapu *et al.* 2016). If there is a substantial overlap of the 90% confidence intervals, it may be assumed that the peak flows are *i.i.d.*, however, the ratio of flood quantiles may indicate otherwise. Therefore, to further evaluate, the ratio of flood quantile of the negative episode to the flood quantile of the positive episode, termed as flood ratio (FR), is computed for selected return periods, 2-, 5-, 10-, 25-, 50- and 100-years (Franks & Kuczera 2002; Gurrapu *et al.* 2016). If the flood ratio is greater than 1 ($FR > 1$), it may be assumed

that the higher magnitude floods are more common during the negative episodes of the teleconnection and vice-versa. While the flood ratio is computed in the same way for evaluating the influence of the ENSO, it is computed as the ratio of flood quantile from La Niña episodes to the quantiles from El Niño episodes to evaluate the effect of ENSO.

RESULTS AND DISCUSSION

This study was motivated by the observation that the influence of low frequency oscillations upon flood risk is not yet a key ingredient in the planning and design of regional infrastructure, despite several studies showing the strong impact of these teleconnections on ISMR. The influence of low-frequency atmosphere-ocean oscillation was first evaluated using a rank-based Spearman's correlation coefficient (ρ) and its statistical significance (p -value) at a 90% confidence interval ($\alpha = 0.05$). First, the peak (annual and seasonal) flows at each gauging station are standardized using Equation (2) and then their correlations with each of the PDO, ENSO and IOD indices are computed.

$$Q_{\text{std},i} = \frac{(Q_i - \bar{Q})}{(Q_{\text{sd}})} \quad (2)$$

where $Q_{\text{std},i}$ is the standardized peak (annual or seasonal) streamflow for the year ' i ', Q_i is the peak (annual or seasonal) streamflow for the year ' i ', \bar{Q} is the mean of the peak (annual or seasonal) flow series and Q_{sd} is the standard deviation of the peak flow series.

Figure 4 presents the Spearman's correlations (Spearman's ρ) between NE monsoon seasonal peak flow (standardized; x -axis) and October to December averaged PDO (PDO_{OND} ; y -axis) in the selected gauging stations from (a) Godavari and (b) Narmada River basins. Eighteen out of 46 selected gauges (i.e. $\approx 39\%$) in the Godavari River basin show statistically significant correlations. In all these stations, the annual peaks are negatively correlated, indicating that the high magnitude floods are more common in the negative phase of PDO when compared to that of the positive phase. These results concur with the observations made by earlier researchers who indicate that the negative phase of PDO produces wet years, i.e. higher ISMR (e.g. Krishnamurthy & Krishnamurthy 2013a). The strength of correlations ranged between -0.25 and -0.5 at all these gauging sites, indicating that as much as 50% of the variability in NE monsoon seasonal peak streamflow can be explained by the low-frequency PDO. In contrast to the Godavari River basin, seasonal peak flow at selected gauging stations from the Narmada River basin does not show as many statistically significant correlations with PDO (Figure 4(b)). Only 2 out of 18 selected gauges show statistically significant correlations. NE monsoon seasonal peak flow at the Chidgaon station (Stn ID: NCHH11) and Garudeshwar (Stn ID: NGAR17) show a negative correlation, in concurrence with the correlations observed at the gauges of the Godavari River basin.

The correlations between annual peak flows and June to December averaged PDO indices ($\text{PDO}_{\text{Jun-Dec}}$) and between SW monsoon seasonal peak flows and June to September averaged PDO indices (PDO_{JJAS}) were also computed. Table 2 lists the strength of correlation (Spearman's ρ) between the standardized annual (WY) and seasonal (SW and NE monsoon) peak flows in the selected gauges and the indices of PDO, ENSO and IOD. The SW monsoon seasonal peak flows in seven gauging stations of the Godavari basin show statistically significant negative correlations with PDO_{JJAS} , whereas no station from the Narmada basin shows a statistically significant correlation. The annual peak flows in nine gauging stations of the Godavari basin show statistically significant negative correlations with $\text{PDO}_{\text{Jun-Dec}}$, whereas only one station from the Narmada basin shows a statistically significant positive correlation with PDO. Annual peak flows at Bamni Banjar (Stn ID: NBAM04) show a positive correlation indicating that the positive episodes of PDO produced higher magnitude peak flows. Although it is generally agreed that the positive phase of PDO produces dry years and the negative phase produces wet years, these relationships deviate moderately along parts of central India, northeastern states, and western and eastern Ghats (Krishnamurthy & Krishnamurthy 2013a). Hence, the contrasting correlation at Bamni Banjar and a few other gauging stations showed a positive correlation, although statistically not significant.

In a similar manner, NE monsoon seasonal streamflow in 20 out of 46 gauging stations ($\approx 43\%$) in the Godavari River basin shows statistically significant negative correlations, indicating that higher magnitude flows are more common during the La Niña episodes of ENSO ($\text{ONI}_{\text{OND}} < -0.5$) (Table 2). The strength of Spearman's ρ correlation ranged between -0.30 and -0.56 , indicating that as much as 56% of the variability in NE monsoon seasonal peak flows at these gauging stations can be explained by the ENSO pattern. Four out of 18 gauging stations ($\approx 22\%$) from the Narmada River Basin show statistically significant correlations. In comparison, only a few gauging stations showed statistically significant correlations with annual

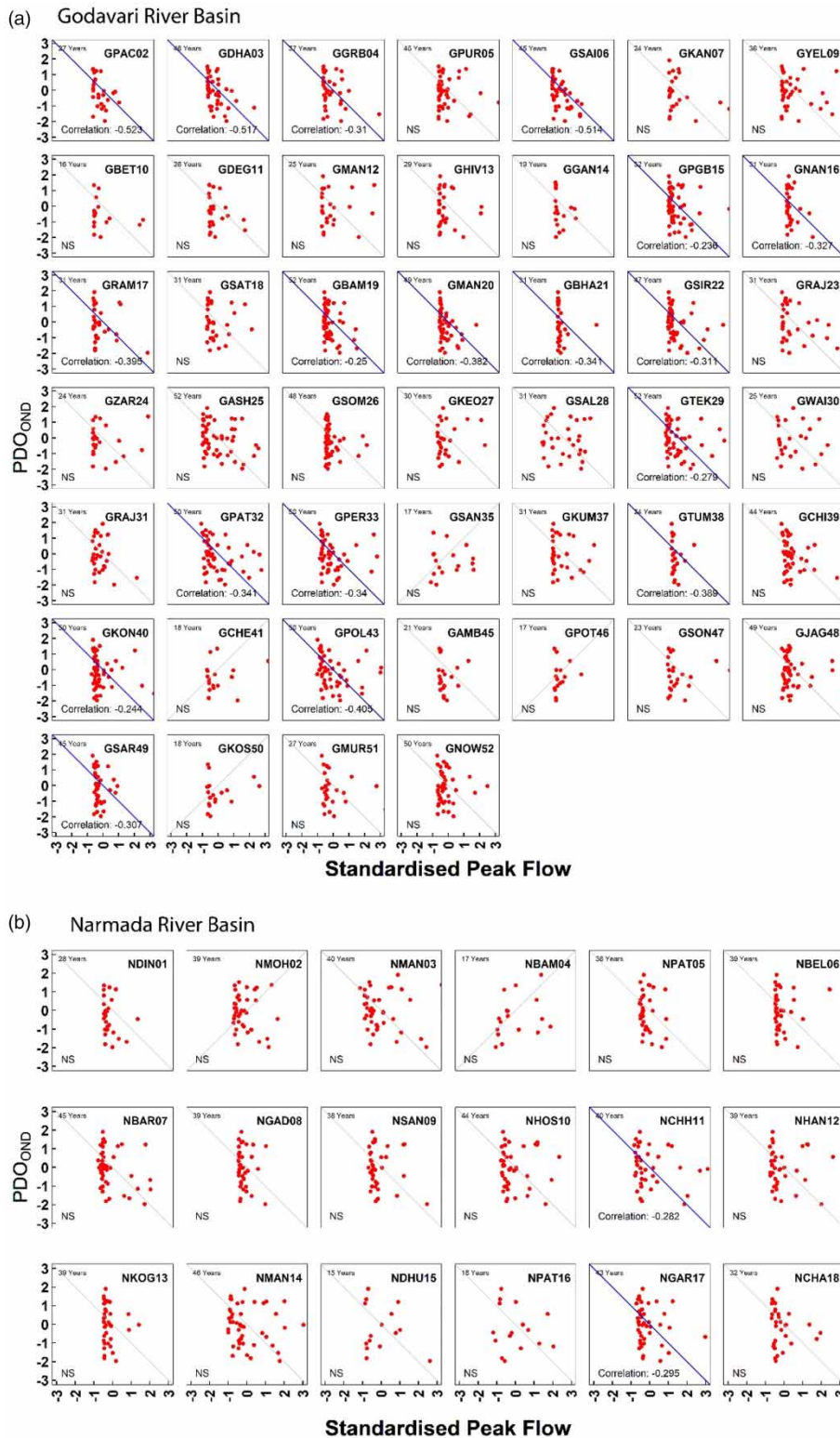


Figure 4 | Rank-based Spearman correlations between NE monsoon seasonal peak flows (standardized; x-axis) and October to December averaged Pacific Decadal Oscillation indices (PDO_{OND}; y-axis) in the selected gauges of (a) Godavari and (b) Narmada River basins. Statistically significant correlations are highlighted with a blue colored 1:1 line and the strength of the correlation is given in the bottom right corner. Station code is indicated in the top right corner and the length of data used is given in the top left corner. Please refer to the online version of this paper to see this figure in colour: <https://dx.doi.org/10.2166/wcc.2023.302>.

Table 2 | Rank-based Spearman correlations between standardized annual (WY), SW monsoon seasonal (SW), NE monsoon seasonal (NE) peak flows and the low-frequency atmosphere-ocean oscillations including Pacific Decadal Oscillation (PDO), El Niño-Southern Oscillation (ENSO) and Indian Ocean Dipole (IOD)

Stn. ID	PDO			ENSO			IOD		
	WY	SW	NE	WY	SW	NE	WY	SW	NE
GPAC02	-0.427	-0.336	-0.523	-0.020	0.010	-0.395	0.277	0.386	-0.402
GDHA03	-0.273	-0.196	-0.517	-0.151	-0.105	-0.479	-0.177	-0.022	-0.449
GGRB04	-0.184	-0.165	-0.310	-0.208	-0.207	-0.314	-0.137	-0.063	-0.431
GPUR05	-0.128	-0.102	-0.122	-0.235	-0.250	-0.354	-0.343	-0.319	-0.451
GSAI06	-0.289	-0.183	-0.514	-0.463	-0.409	-0.561	-0.371	-0.159	-0.569
GKAN07	-0.155	-0.126	-0.207	-0.205	-0.263	-0.239	-0.136	-0.145	-0.344
GYEL09	-0.034	0.070	-0.131	-0.167	-0.091	-0.476	-0.178	-0.054	-0.544
GBET10	0.012	0.106	-0.094	-0.294	-0.415	-0.196	-0.476	-0.468	-0.468
GDEG11	0.074	-0.019	-0.185	-0.306	-0.404	-0.194	-0.269	-0.291	-0.316
GMAN12	-0.163	-0.163	-0.025	0.037	0.002	-0.191	0.115	-0.039	-0.212
GHIV13	-0.392	-0.402	-0.020	-0.014	-0.051	-0.188	0.245	0.166	-0.237
GGAN14	-0.263	-0.358	-0.374	-0.388	-0.405	-0.458	-0.157	-0.027	-0.265
GPGB15	-0.054	-0.064	-0.236	-0.227	-0.229	-0.495	-0.165	-0.180	-0.293
GNAN16	-0.458	-0.432	-0.327	-0.159	-0.172	-0.275	0.084	0.137	-0.183
GRAM17	-0.093	-0.068	-0.395	0.196	0.235	-0.261	0.158	0.055	-0.310
GSAT18	-0.121	-0.079	-0.214	0.137	0.109	-0.155	0.163	0.110	-0.247
GBAM19	0.024	0.003	-0.250	-0.086	-0.056	-0.479	0.137	0.084	-0.181
GMAN20	-0.132	-0.124	-0.382	-0.355	-0.314	-0.501	-0.245	-0.244	-0.318
GBHA21	-0.242	-0.177	-0.341	-0.353	-0.314	-0.413	-0.142	-0.188	-0.256
GSIR22	-0.154	-0.122	-0.311	-0.143	-0.174	-0.418	-0.004	-0.015	-0.102
GRAJ23	-0.314	-0.279	-0.206	-0.055	-0.080	-0.223	0.158	0.197	-0.066
GZAR24	0.049	0.002	-0.012	-0.155	-0.312	-0.150	-0.463	-0.453	-0.386
GASH25	-0.325	-0.275	-0.217	-0.283	-0.315	-0.306	-0.067	-0.046	-0.172
GSOM26	0.014	0.019	-0.033	-0.264	-0.200	-0.347	-0.198	-0.136	-0.231
GKEO27	-0.169	-0.135	-0.079	-0.074	-0.104	-0.069	0.040	-0.002	-0.196
GSAL28	-0.068	-0.091	-0.108	-0.161	-0.217	-0.335	-0.002	-0.057	-0.422
GTEK29	-0.191	-0.171	-0.279	-0.204	-0.215	-0.442	0.082	0.114	-0.159
GWAI30	-0.515	-0.522	-0.058	-0.036	-0.109	-0.087	0.281	0.268	-0.053
GRAJ31	-0.136	-0.113	-0.150	0.008	-0.007	-0.067	0.043	-0.046	-0.239
GPAT32	-0.162	-0.082	-0.341	0.069	0.029	-0.372	0.069	0.009	-0.101
GPER33	-0.214	-0.148	-0.340	-0.245	-0.236	-0.511	0.006	-0.017	-0.232
GSAN35	0.194	0.355	0.044	-0.044	-0.045	-0.199	-0.387	-0.451	-0.301
GKUM37	-0.310	-0.340	-0.254	0.017	0.032	-0.187	0.105	0.003	-0.247
GTUM38	-0.171	0.038	-0.389	-0.231	-0.120	-0.273	-0.100	-0.088	0.004
GCHI39	-0.167	-0.100	-0.247	0.113	0.150	-0.226	0.086	0.004	-0.131
GKON40	-0.085	-0.016	-0.244	-0.046	-0.021	-0.302	-0.091	-0.124	-0.140
GCHE41	0.104	0.129	0.030	0.226	0.198	0.040	0.335	0.240	0.020
GPOL43	-0.105	0.002	-0.405	-0.200	-0.173	-0.540	-0.033	-0.054	-0.246
GAMB45	0.008	0.058	-0.152	0.051	-0.008	-0.274	0.090	-0.005	-0.022
GPOT46	0.110	0.145	0.176	-0.042	0.072	-0.069	0.270	0.240	-0.130
GSON47	0.065	0.136	-0.161	-0.135	-0.070	-0.213	-0.088	-0.068	-0.198
GJAG48	0.073	0.021	-0.104	0.136	0.091	-0.121	-0.090	-0.150	-0.118
GSAR49	-0.102	-0.064	-0.307	0.084	0.106	-0.211	0.049	-0.088	-0.193
GKOS50	0.051	0.208	0.001	0.081	-0.006	-0.023	0.214	0.022	-0.034
GMURS1	-0.168	-0.053	-0.207	0.111	0.027	0.098	0.036	-0.004	-0.054
GNOW52	0.075	0.083	-0.048	0.085	0.151	0.066	-0.054	-0.103	0.055
NDIN01	0.183	0.217	-0.177	0.098	0.136	0.067	-0.029	-0.048	-0.066
NMOH02	0.071	0.108	0.003	0.082	0.175	-0.063	-0.053	-0.082	-0.083
NMAN03	0.137	0.184	-0.162	0.039	0.109	-0.036	0.014	-0.046	-0.092
NBAM04	0.441	0.365	0.382	0.399	0.259	0.315	-0.147	-0.476	-0.007
NPAT05	-0.031	-0.056	-0.128	0.012	0.143	-0.011	0.108	0.106	-0.131
NBEL06	0.083	-0.001	-0.245	0.172	0.222	-0.141	0.244	0.222	-0.320
NBAR07	-0.118	-0.206	-0.183	-0.030	-0.002	-0.130	0.052	0.019	-0.194
NGAD08	-0.094	-0.165	-0.215	0.077	0.074	-0.135	0.200	0.188	-0.193
NSAN09	-0.044	-0.119	-0.116	0.087	0.184	-0.152	0.183	0.144	-0.170
NHOS10	-0.110	-0.188	-0.097	-0.079	-0.038	-0.123	0.097	0.073	-0.193
NCHH11	-0.087	-0.022	-0.282	-0.026	0.086	-0.268	-0.010	0.038	-0.302
NHAN12	-0.115	-0.219	-0.172	0.105	0.111	-0.197	0.103	0.087	-0.261
NKOG13	0.062	0.059	-0.231	0.226	0.206	-0.457	0.089	0.065	-0.545
NMAN14	-0.109	-0.125	-0.211	0.032	0.038	-0.304	0.108	0.120	-0.248
NDHU15	0.218	0.194	-0.111	0.250	0.246	-0.147	-0.100	-0.159	-0.400
NPAT16	-0.179	-0.226	-0.176	-0.184	-0.221	-0.027	-0.165	0.021	-0.153
NGAR17	-0.108	-0.113	-0.295	-0.122	-0.130	-0.383	-0.030	-0.033	-0.448
NCHA18	-0.158	-0.054	-0.158	-0.163	-0.106	-0.110	-0.098	-0.063	-0.080

The statistically significant ($\alpha = 0.1$) correlations are bolded, and the negative (positive) statistically significant correlations are shaded in blue (red).

and SW monsoon seasonal peak flows, i.e. 7 each for the Godavari River basin and none for the Narmada River basin. All these correlations are negative, indicating that higher magnitude floods have occurred during the La Niña episodes of ENSO.

The correlations between IOD and annual peak flows are statistically significant and negative in four gauging stations in the Godavari basin and none in the Narmada basin. Whereas the correlations between IOD and SW monsoon seasonal peak flow are statistically significant in five (four negative and one positive) gauging stations of Godavari and one (negative) in the Narmada basin. The signal of IOD is strongly seen in the NE monsoon seasonal peak flows, similar to the other teleconnections, 13 out of 46 gauging stations (28%) in the Godavari basin and 4 out of 18 stations (22%) in the Narmada basin show statistically significant negative correlations, indicating that higher magnitude floods are more common during the negative episodes of IOD. Overall, the NE monsoon seasonal peak flows indicate a strong signal of PDO, ENSO and IOD, and all these correlations indicate that higher magnitude floods are common during the negative episodes of these teleconnections (Table 2).

To further evaluate the influence of teleconnections on annual floods, Q-Q plots are constructed after stratifying the annual and seasonal peak flow as a response to the episodes (positive or negative) of each teleconnection. Figure 5 demonstrates, through Q-Q plots, the influence of PDO on NE monsoon seasonal peak flows in the selected gauging stations from across the Godavari River basin. These plots confirm that it is unlikely that the annual peak flows are identically distributed regardless of the strength of the PDO episode since there are few gauges where the quantiles fall along the 1:1 line. The Q-Q plots illustrate that higher magnitude flows are typically more common during the negative phase of PDO since the flood quantiles largely appear above the 1:1 line. The permutation tests show that this is a significant result ($p < 0.1$) for 17 out of the 39 records, i.e. more than 40% of the gauges indicate that the higher magnitude floods occurred in response to the negative PDO episodes (Figure 5). In the Narmada River basin, 4 out of 18 gauging stations show statistically significant relationships indicating that higher magnitude floods occurred in response to the negative PDO episodes. Overall, NE monsoon seasonal floods in 21 out of 64 gauging stations ($\approx 33\%$) are higher in magnitude during the negative episodes of PDO (i.e. $\text{PDO}_{\text{OND}} \leq -0.05$) (Table 3).

The Q-Q plots are also constructed to evaluate the relationships between the ENSO and IOD and annual and seasonal peak flows in all the selected gauging stations. These Q-Q plots were tested for statistical significance at a 90% confidence interval ($\alpha = 0.1$), two-sided. Table 3 lists the negative (-ve) and positive (+ve) episodes of a teleconnection, i.e. PDO, ENSO and IOD, in which higher magnitude annual (WY) and/or seasonal (SW and NE) floods may be expected, based on the statistically significant Q-Q plots. In summary, 17 stations indicate higher magnitude annual floods, and 14 stations indicate higher magnitude SW monsoon seasonal floods in response to negative PDO episodes. On the contrary, one station indicates higher magnitude annual floods, and three stations indicate higher magnitude SW monsoon seasonal floods in response to the positive episodes of PDO. The ENSO signal indicates that 16 stations show higher magnitude annual floods, 25 stations show higher magnitude SW monsoon seasonal floods and 25 stations show higher magnitude NE monsoon seasonal floods in response to La Niña episodes. Similarly, four stations show higher magnitude annual floods, five stations show higher magnitude SW monsoon seasonal floods and 29 stations show higher magnitude floods in response to the negative episodes of the IOD. Only a few stations ($\leq 7.5\%$) indicate that higher magnitude floods occur in response to positive episodes of these teleconnections. Overall, the NE monsoon seasonal floods show a clear signal of PDO (21 out of 64 or $\approx 33\%$), ENSO (25 out of 64 or $\approx 39\%$) and IOD (29 out of 64 or $\approx 45\%$), all indicating that higher magnitude floods occur in response to the negative episodes of these teleconnections (Table 3). These results are in agreement with the earlier observations made, i.e. negative episodes of these teleconnections produce wetter years (e.g. Krishnamurthy & Krishnamurthy 2013a; Saini *et al.* 2022).

To further evaluate, flood frequency curves are constructed to the stratified annual and seasonal peak flow data. Figure 6 presents the flood frequency curves for four gauging stations spread across the Godavari River basin, the curves fit the NE monsoon seasonal floods stratified based on the positive (red curves) and negative (blue curves) episodes of PDO. Three of the stations (a, c and d) are regulated and the other station (b) is located on the naturally flowing streams. All four stations clearly indicate that the hydrological response of the watershed in both phases of PDO is distinctly different. The flood frequency curves (red and blue) separate clearly indicating that the NE monsoon seasonal floods are not identically distributed. Also, there is clear evidence that higher magnitude floods are more common during the negative phase of PDO. Although not all the gauges show a clear separation of flood frequency curves, the majority of the gauges illustrate the influence of PDO on the distribution of seasonal peak flows. Irrespective of whether the flow gauging station is on a naturally flowing or on a regulated stream, the flood frequency curves show a clear signal of PDO. Similarly, the gauges of the Narmada River basin

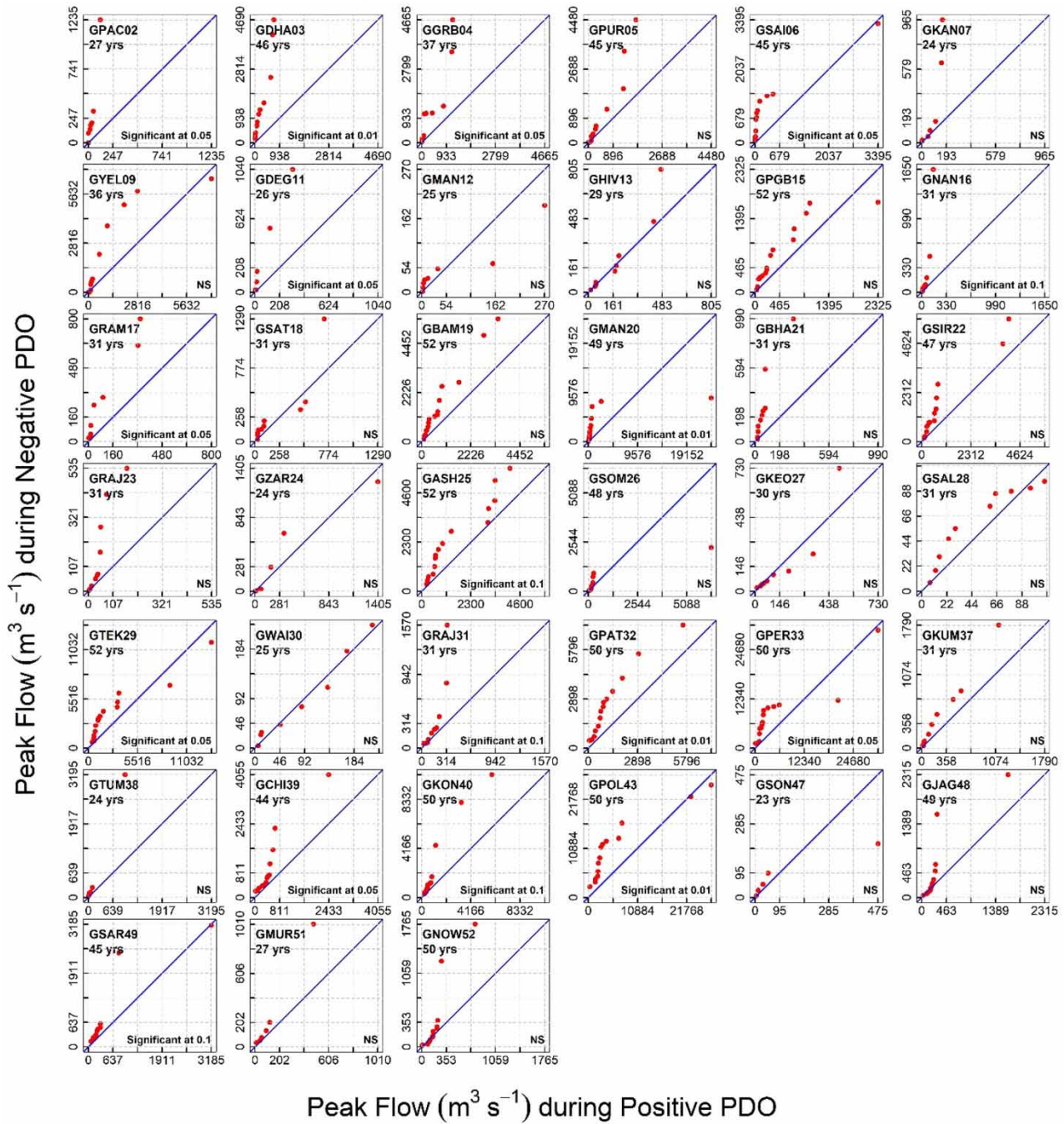


Figure 5 | Quantile-Quantile plots based on NE monsoon seasonal peak flows (m^3/s) stratified according to the positive and negative episodes of Pacific Decadal Oscillations (PDO) for the selected streamflow gauging stations in the Godavari River basin. Shown in blue are the 1:1 lines. The station codes are shown in the upper left-hand corners, together with record length. Shown in the lower right corner are the statistical significance levels of the permutations test. NS indicates statistically not significant. Please refer to the online version of this paper to see this figure in colour: <https://dx.doi.org/10.2166/wcc.2023.302>.

indicate a negative influence on the seasonal peak flows, i.e. higher magnitude flows during the negative phase of PDO and vice-versa (results not presented). Despite the overlap of confidence intervals for a few gauging stations, the flood frequency curves demonstrate that higher magnitude floods are commonly observed in response to the negative episodes of PDO. A similar separation in flood frequency curves is observed when analyzed for the annual and SW monsoon seasonal peak

Table 3 | Negative (–ve) and positive (+ve) episodes of teleconnections, namely, PDO, ENSO and IOD, indicative of higher magnitude annual (WY), southwest monsoon seasonal (SW), northeast monsoon seasonal (NE) peak flows or floods

Stn_ID	PDO			ENSO			IOD		
	WY	SW	NE	WY	SW	NE	WY	SW	NE
GPAC02	- ve	- ve	- ve	-	-	- ve	+ ve	+ ve	- ve
GDHA03	- ve	- ve	- ve	-	- ve	- ve	-	-	- ve
GGRB04	-	-	- ve	-	- ve	- ve	-	-	- ve
GPUR05	-	-	-	-	- ve	- ve	- ve	-	- ve
GSAI06	- ve	- ve	- ve	- ve	- ve	- ve	-	-	- ve
GKAN07	-	- ve	-	-	- ve	-	-	-	- ve
GYEL09	-	-	-	- ve	- ve	- ve	-	-	- ve
GBET10	-	-	-	-	-	-	- ve	- ve	- ve
GDEG11	-	-	- ve	- ve	- ve	-	-	- ve	-
GMAN12	-	-	-	-	- ve	-	-	-	-
GHIV13	- ve	- ve	-	- ve	- ve	-	-	-	-
GGAN14	- ve	- ve	-	- ve	- ve	- ve	-	-	-
GPGB15	-	-	-	- ve	- ve	- ve	-	-	- ve
GNSN16	- ve	- ve	- ve	-	- ve	-	-	-	-
GRAM17	-	-	- ve	-	-	-	-	-	- ve
GSAT18	-	-	-	-	-	-	-	-	- ve
GBAM19	-	-	-	- ve	- ve	- ve	-	-	- ve
GMAN20	- ve	- ve	- ve	- ve	- ve	- ve	-	-	- ve
GBHA21	- ve	- ve	-	- ve	- ve	- ve	-	-	-
GSIR22	-	-	-	- ve	- ve	- ve	-	-	- ve
GRAJ23	-	-	-	-	- ve	-	-	-	-
GZAR24	-	-	-	-	-	-	- ve	- ve	- ve
GASH25	- ve	- ve	- ve	- ve	- ve	- ve	-	-	-
GSOM26	-	-	-	- ve	- ve	-	-	-	-
GKEO27	-	-	-	-	- ve	-	-	-	- ve
GSAL28	-	-	-	-	- ve	- ve	-	-	- ve
GTEK29	-	-	- ve	-	-	- ve	-	-	-
GWAI30	- ve	- ve	-	-	-	-	+ ve	-	-
GRAJ31	-	- ve	- ve	- ve	- ve	-	-	-	-
GPAT32	- ve	-	- ve	-	-	- ve	-	-	-
GPFR33	- ve	-	- ve	-	- ve	- ve	-	-	-
GSAN35	-	-	-	-	-	-	- ve	- ve	- ve
GKUM37	- ve	- ve	-	- ve	-	-	-	-	-
GTUM38	-	-	-	-	-	- ve	-	-	-
GCHI39	- ve	-	- ve	-	-	- ve	-	-	-
GKON40	-	-	- ve	-	- ve	- ve	-	-	-
GCHE41	-	-	-	-	-	-	+ ve	-	-
GPOL43	-	-	- ve	- ve	- ve	- ve	-	-	-
GAMB45	-	-	-	-	-	-	-	-	-
GPOT46	-	-	-	-	-	-	+ ve	-	-
GSON47	-	-	-	-	-	-	-	-	- ve
GJAG48	-	-	-	+ ve	-	-	-	-	- ve
GSAR49	- ve	-	- ve	-	-	-	-	-	-
GKOS50	-	-	-	-	-	-	+ ve	-	-
GMUR51	-	-	-	-	-	-	-	-	-
GNOW52	-	-	-	-	-	-	-	-	- ve
NDIN01	-	+ ve	-	-	-	-	-	-	-
NMOH02	-	-	-	- ve	-	-	-	-	-
NMAN03	- ve	+ ve	- ve	-	-	-	-	-	-
NBAM04	-	-	-	+ ve	-	-	-	-	-
NPAT05	- ve	- ve	-	-	-	-	-	-	-
NBEL06	-	-	-	-	-	-	-	-	- ve
NBAR07	-	-	-	-	-	-	-	-	-
NGAD08	-	-	- ve	-	-	-	-	-	-
NSAN09	-	-	-	-	- ve	-	-	-	- ve
NHOS10	-	-	-	-	-	-	-	-	-
NCHH11	-	-	- ve	-	-	-	-	-	- ve
NHAN12	-	-	-	-	-	-	-	-	- ve
NKOG13	-	-	-	-	-	- ve	-	-	- ve
NMAN14	-	-	-	-	-	- ve	-	-	- ve
NDHU15	+ ve	+ ve	-	-	-	-	-	- ve	- ve
NPAT16	-	-	-	-	-	-	-	-	-
NGAR17	-	-	- ve	-	-	- ve	-	-	- ve
NCHA18	-	-	-	-	-	- ve	-	-	-

These relations are based on the statistically significant ($\alpha = 0.1$) Q-Q plots, e.g. Figure 5. The symbol ‘-’ indicates a statistically insignificant Q-Q plot. The negative (positive) statistically significant correlations are shaded in blue (red).

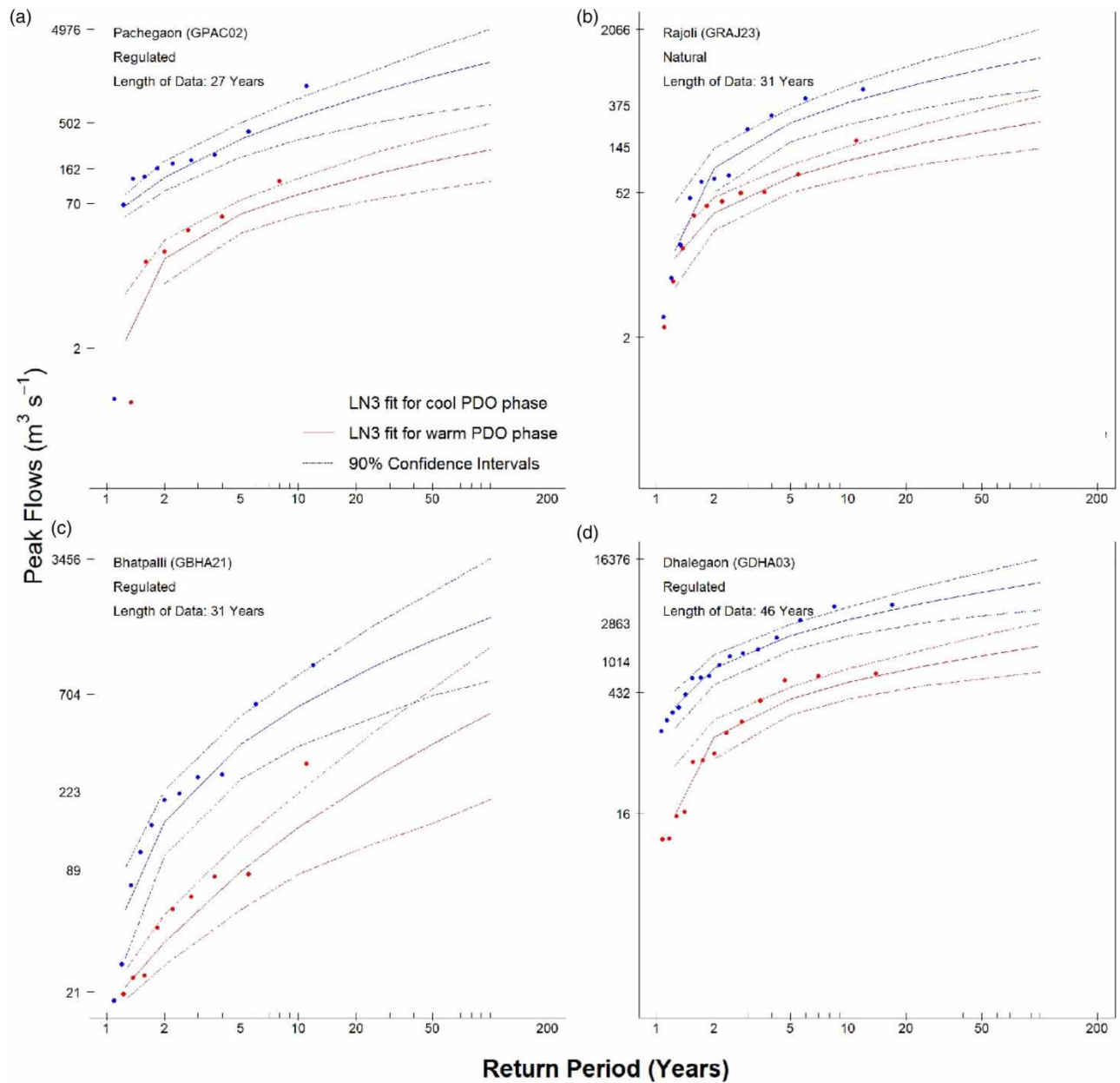


Figure 6 | 3-Parameter Lognormal (LN3) flood frequency curves (solid lines) and their 90% confidence intervals (dashed lines) for the NE monsoon seasonal peak flows in selected gauges of the Godavari River basin, stratified according to negative ($PDO_{OND} \leq -0.5$) and positive ($PDO_{OND} \geq 0.5$) episodes of Pacific Decadal Oscillation (PDO). (a) Pachhegaon, (b) Rajoli, (c) Bhatpalli and (d) Dhalegaon. Please refer to the online version of this paper to see this figure in colour: <https://dx.doi.org/10.2166/wcc.2023.302>.

flows. Overall, the selected gauging stations indicate that annual and seasonal peak flows are substantially influenced by the phase of PDO.

In a similar way, the influence of ENSO and IOD on flood frequency is also analyzed and in a majority of the gauging stations, the flood frequency curves separate. Figures 7(a) and 7(b) demonstrate the influence of ENSO on flood frequency and Figures 7(c) and 7(d) demonstrate the influence of IOD on flood frequency. The flood frequency curves fit the 3-parameter lognormal distribution along with 90% confidence intervals clearly indicating that there is a substantial difference between flood magnitude and frequency based on the phases (negative and positive) of ENSO and IOD at these gauging stations. These curves clearly indicate that the higher magnitude floods generally occurred during the negative episodes of ENSO and IOD.

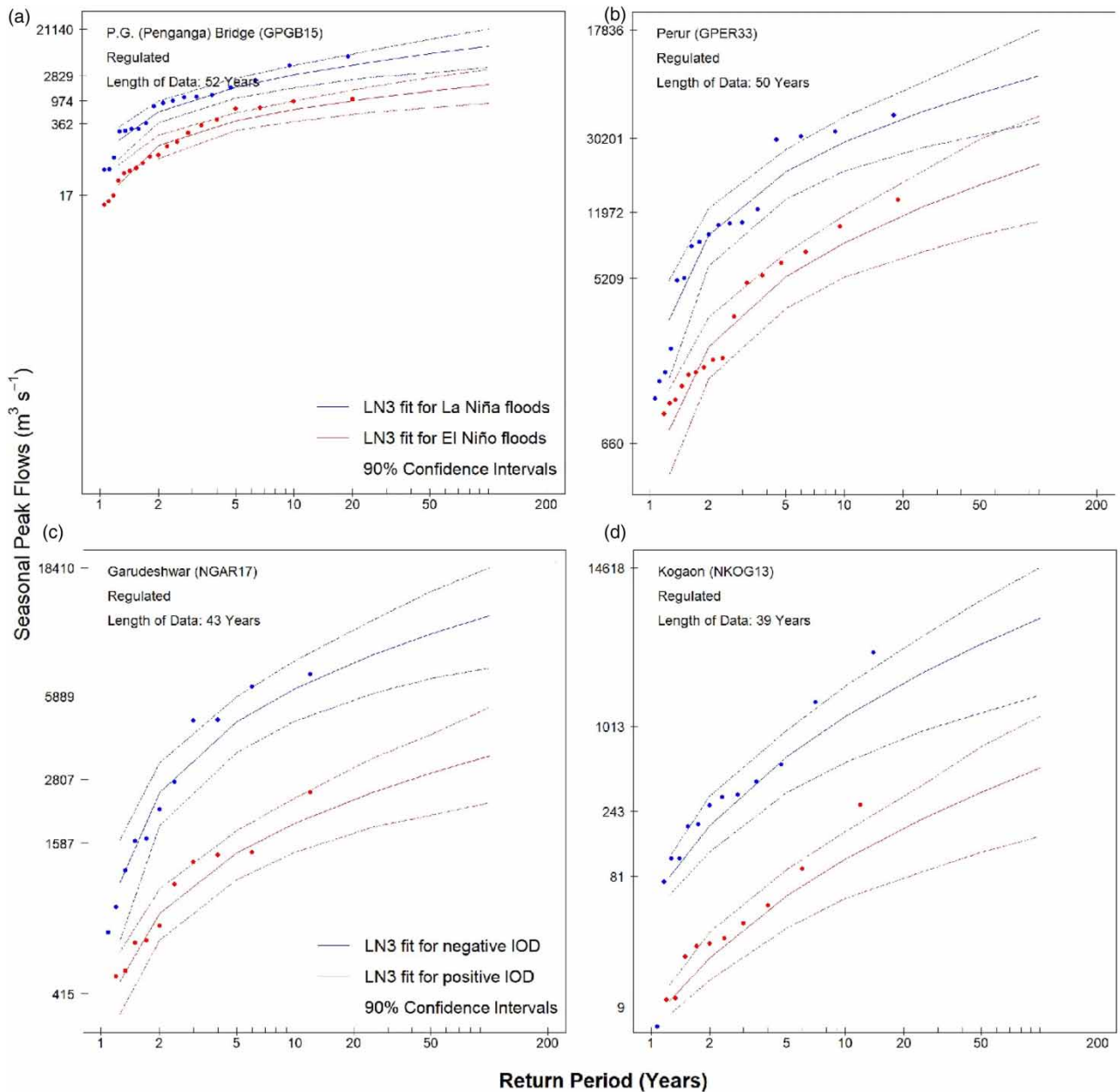


Figure 7 | 3-Parameter Lognormal (LN3) flood frequency curves (solid lines) and their 90% confidence intervals (dashed lines) for the northeast monsoon seasonal (NE) peak flows in two selected gauges from the Godavari River basin, (a) P.G. (Penganga) Bridge, (b) Perur, stratified according to El Niño ($ONI_{OND} \geq -0.5$) and La Niña ($ONI_{OND} \leq -0.5$) episodes of El Niño-Southern Oscillation (ENSO) pattern and in two selected gauges from the Narmada River basin, (c) Garudeshwar and (d) Kogaon, stratified according to positive ($DMI_{OND} \geq 0.1$) and negative ($DMI_{OND} \leq -0.1$) episodes of Indian Ocean Dipole (IOD).

As only a few gauges show a clear separation of the flood frequency curves stratified based on the phases of low-frequency oscillations, flood ratio analysis is adopted to evaluate the regional impact of these oscillations. Using the flood quantiles estimated through flood frequency analysis (FFA), the flood ratio is computed for each gauging station at several return periods (Figure 8). If the peak flows are independent and identically distributed, at least 50% of the selected gauges would have a flood ratio (FR) ≤ 1 . Figure 8(a) illustrates the histogram of flood ratios (at various return periods) of 46 gauges spread across the Godavari River basin to show the impact of IOD. This figure clearly indicates that the flood ratio is more than 1 in more than 70% of the gauges for all the return periods. For at least 40% of the selected gauges, this ratio is higher

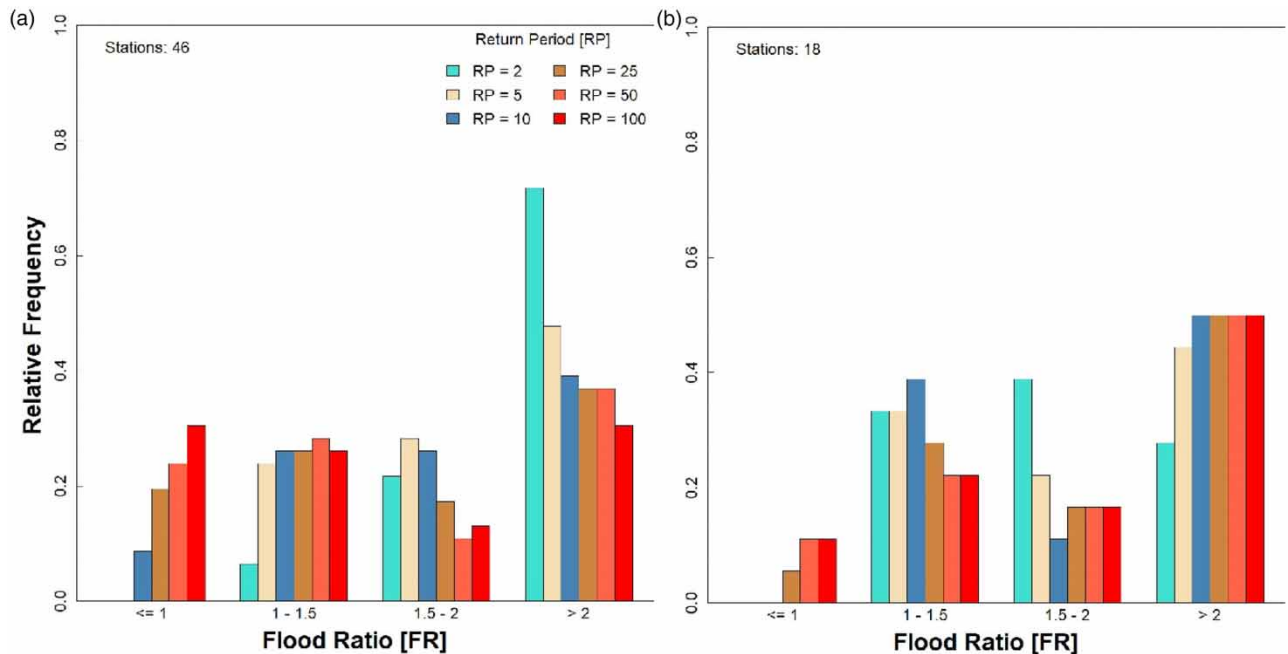


Figure 8 | Histogram of flood ratios (FR) for return periods between 2 and 100 years for the (a) 46 gauges spread across the Godavari River basin and (b) 18 gauges spread across the Narmada River basin. FR is the ratio of flood quantiles in negative and positive episodes of IOD, extracted after fitting the stratified northeast monsoon seasonal (NE) peak flow data to a 3-parameter lognormal distribution.

than 1.5, which is a very strong evidence of the impact of IOD. At return periods, 2 and 5, the flood ratio is greater than 1 in 100% of the gauging stations, a clear signal of IOD. Similarly, Figure 8(b) presents the histogram of flood ratios of 18 gauges spread across the Narmada River basin. This figure illustrates that more than 80% of the gauging stations show a flood ratio greater than 1, indicating that higher magnitude floods may be expected in response to the negative episodes of IOD. At return periods 2, 5 and 10, the flood ratio is much higher than 1 in 100% of the gauging stations, clear evidence of teleconnection. Both Figures 8(a) and 8(b) indicate that higher magnitude floods of NE monsoon season are common during the negative episodes of IOD in both basins.

The regional influence of PDO and ENSO on annual and seasonal peak flows is also analyzed using the flood ratio approach, results not presented. The annual floods fail to show the signal of either of the teleconnections, i.e. PDO, ENSO or IOD, because the flood ratio is less than or equal to 1 in nearly 50% of the stations and is more than 1 in the other half, for most of the return periods. However, floods with higher frequency (i.e. $RP = 2$ or 5) indicate that higher magnitude floods are marginally higher during the negative episodes ($FR > 1$ in nearly 60% of the stations) of PDO and IOD. The regional influence of ENSO on annual peak flows in the gauges of the Narmada River basin is not distinctly seen using the flood ratio approach. In contrast, the influence of all these teleconnections is clearly seen on NE monsoon seasonal floods, indicating that higher magnitude floods are more common during the negative episodes of PDO, ENSO and IOD.

CONCLUSIONS

The return period or frequency of a flood event is one key piece of information required for adequate planning and design of water resources infrastructure and for effective management of available water. Traditionally, such information is obtained from FFA, which assumes that the annual peak flow series is independent and identically distributed (*i.i.d.*). Almost all the FFA done in India invokes the assumption of *i.i.d.* and this study aimed to evaluate its competency in making estimates of the design flood. The results indicate that the annual and seasonal peak flows in the gauges spread across the Godavari and Narmada River basins indicate that their magnitude and frequency are substantially influenced by the phases of PDO, ENSO or IOD. In particular, the influence of these teleconnections is clearly seen on the seasonal, namely, northeast (NE) and southwest (SW) monsoon, peak flows. In the majority of the gauges, higher magnitude floods seem to be more common during the negative episodes of PDO, ENSO (La Niña) or IOD. In addition, the regional influence of these

teleconnections is seen in the magnitude and frequency of seasonal peak flows using the flood ratio approach. The signal of these teleconnections is clearly seen in the seasonal floods of higher frequency (i.e. RP = 2, 5 and 10 years), where almost all the gauging stations indicate that the higher magnitude floods are common during negative episodes. Overall, the results from this study highlight the potential inadequacy of the *i.i.d.* assumption and are not tenable where the hydroclimatology is strongly influenced by the low-frequency atmosphere-ocean oscillations. These results are in agreement with the observations made by other researchers across the globe (e.g. Kwon *et al.* 2008; Stedinger & Griffis 2008, 2011; López & Francès 2013; Barros *et al.* 2014; Gurrapu *et al.* 2016). This is manifest in the Godavari and Narmada River basins in India and other parts across the globe including western Canada, California and eastern Australia (e.g. this study; Franks & Kuczera 2002; Ward *et al.* 2014; Gurrapu *et al.* 2016). The extent of this problem in other Indian watersheds remains to be explored. Any region with a strong teleconnection with such large-scale atmosphere-ocean oscillations may be subject to under- or over-estimation of the design flood. Therefore, the knowledge of the regional hydroclimate with regards to phases of the large-scale low-frequency atmosphere-ocean oscillations should be considered prior to estimating the design flood. Furthermore, the effect of other atmosphere-ocean oscillations, e.g. North Atlantic Oscillation (NAO), Arctic Oscillation (AO) and Atlantic Multi-Decadal Oscillation (AMO), on extreme hydrology of Indian watersheds needs to be explored.

DATA AVAILABILITY STATEMENT

All relevant data are available from an online repository or repositories.

Streamflow: (<https://indiawris.gov.in/wris/#/DataDownload>).

PDO: (<http://jisao.washington.edu/pdo/>)

ENSO: (<https://psl.noaa.gov/data/correlation/oni.data>).

IOD: (www.bom.gov.au/climate/iod/)

CONFLICT OF INTEREST

The authors declare there is no conflict.

REFERENCES

- Andrews, E. D., Antweiler, R. C., Neiman, P. J. & Ralph, F. M. 2004 Influence of ENSO on flood frequency along the California Coast. *Journal of Climate* **17** (2), 337–348. doi:10.1175/1520-0442(2004)017%3C0337:IOEOFF%3E2.0.CO;2.
- Barros, A. P., Duan, Y., Brun, J. & Medina, M. A. 2014 Flood non-stationarity in the SE and Mid-Atlantic regions of the United States. *Journal of Hydrologic Engineering* **19** (10), 05014014. doi:10.1061/(ASCE)HE.1943-5584.0000955.
- Bhattacharya, S. & Das, A. 2007 *Vulnerability to Drought, Cyclones, and Floods in India*. The BASIC Project Paper 9. Winrock International, India, p. 43.
- Franks, S. W. 2002 Identification of a change in climate state using regional flood data. *Hydrology and Earth System Sciences* **6** (1), 11–16. doi:10.5194/hess-6-11-2002.
- Franks, S. W. & Kuczera, G. 2002 Flood frequency analysis: evidence and implications of secular climate variability, New South Wales. *Water Resources Research* **38** (5), 20.1–20.7. doi:10.1029/2001WR000232.
- Gurrapu, S., St-Jacques, J. M., Sauchyn, D. J. & Hodder, K. R. 2016 The influence of the Pacific Decadal Oscillation on annual floods in the rivers of Western Canada. *Journal of the American Water Resources Association* **52** (5), 1031–1045. doi:10.1111/1752-1688.12433.
- Gurrapu, S., Sauchyn, D. J. & Hodder, K. R. 2022 Assessment of the hydrological drought risk in Calgary, Canada using weekly river flows of the past millennium. *Journal of Water and Climate Change*. doi:10.2166/wcc.2022.348.
- Helsel, D. R. & Hirsch, R. M. 2002 Statistical methods in water resources (Chapter A3). In: *Book 4 – Hydrologic Analysis and Interpretation*. Techniques of Water-Resources investigations Reports, United States Geological Survey (USGS), Reston, VA.
- Kiem, A. S., Franks, S. W. & Kuczera, G. 2003 Multi-decadal variability of flood risk. *Geophysical Research Letters* **30** (2), 1035. doi:10.1029/2002GL015992.
- Krishnamurthy, L. & Krishnamurthy, V. 2013a Influence of PDO on South Asian Summer Monsoon and Monsoon-ENSO Relation. COLA Technical Report # 321. Centre for Ocean-Land-Atmosphere Studies. Institute of Global Environment & Society, Maryland, USA, p. 41.
- Krishnamurthy, L. & Krishnamurthy, V. 2013b Decadal Scale Oscillation and Trend in the Indian Monsoon Rainfall. COLA Technical Report # 322. Centre for Ocean-Land-Atmosphere Studies. Institute of Global Environment & Society, Maryland, USA, p. 39.
- Kwon, H.-H., Brown, C. & Lall, U. 2008 Climate informed flood frequency analysis and prediction in Montana using hierarchical Bayesian modelling. *Geophysical Research Letters* **35** (5), L05404. doi:10.1029/2007GL032220.
- Li, Z., Lin, X. & Cai, W. 2017 Realism of modelled Indian summer monsoon correlation with the tropical Indo-Pacific affects projected monsoon changes. *Scientific Reports* **7**, 4929. doi:10.1038/s41598-017-05225-z.

- López, J. & Francès, F. 2013 Non-stationary flood frequency analysis in continental Spanish rivers, using climate and reservoir indices as external covariates. *Hydrology and Earth System Sciences* **17** (8), 3189–3203. doi:10.5194/hess-17-3189-2013.
- Manly, B. F. J. 2007 *Randomization, Bootstrap and Monte Carlo Methods in Biology*, 3rd edn. Chapman and Hall, London.
- Mantua, N. J., Hare, S. R., Zhang, Y., Wallace, J. M. & Francis R. C. 1997 A pacific interdecadal climate oscillation with impacts on salmon production. *Bulletin of the American Meteorological Society* **78** (6), 1069–1079. 10.1175/1520-0477(1997)078<1069:APICOW>2.0.CO;2.
- Milly, P. C. D., Betancourt, J., Falkenmark, M., Hirsch, R. M., Kundzewicz, Z. W., Lettermaier, D. P. & Stouffer, R. J. 2008 Stationarity is dead: whither water management. *Science* **319** (5863), 573–574. doi:10.1126/science.1151915.
- Mishra, V., Aaadhar, S., Shah, H., Kumar, R., Pattanaik, D. R. & Tiwari, A. D. 2018 The Kerala flood of 2018: combined impact of extreme rainfall and reservoir storage. *Hydrology and Earth System Sciences*. doi:10.5194/hess-2018-480.
- Roy, S. S., Goodrich, G. B. & Balling Jr., R. C. 2003 Influence of El Niño/Southern Oscillation, Pacific Decadal Oscillation and local sea-surface temperature anomalies on peak season monsoon precipitation in India. *Climate Research* **25** (2), 171–178. doi:10.3354/cr025171.
- Saini, D., Bharadwaj, P. & Singh, O. 2022 Recent rainfall variability over Rajasthan, India. *Theoretical and Applied Climatology* **148** (1–2), 1–19. doi:10.1007/s00704-21-03904-6.
- Sajani, S., Beegum, S. N. & Moorthy, K. K. 2007 The role of low-frequency intraseasonal oscillation in the anomalous Indian summer monsoon rainfall of 2002. *Journal of Earth System Science* **116** (2), 149–157. doi:10.1007/s12040-007-0015-5.
- Saji, N. H., Goswami, B. N., Vinayachandran, P. N. & Yamagata, T. 1999 A dipole mode in the tropical Indian Ocean. *Nature* **401**, 360–363. doi:10.1038/46854.
- Stedinger, J. R. & Griffis, V. W. 2008 Flood frequency analysis in the United States: time to update. *Journal of Hydrologic Engineering* **13** (4), 199–204. doi:10.1061/(ASCE)1084-0699(2008)13:4(199).
- Stedinger, J. R. & Griffis, V. W. 2011 Getting from here to where? Flood frequency and climate. *Journal of the American Water Resources Association* **47** (3), 506–513. doi:10.1111/j.1752-1688.2011.00545.x.
- USGS 1982 *Guidelines for Determining Flood Flow Frequency*. *Bulletin 17B of the Hydrology Subcommittee*. United States Geological Survey (USGS), Reston, VA. Available at: http://water.usgs.gov/osw/bulletin17b/dl_flow.pdf.
- Walker, G. 1933 Seasonal weather and its prediction. *Nature* **132**, 805–808. doi:10.1038/132805a0.
- Ward, P. J., Eisner, S., Florke, M., Dettinger, M. D. & Kummerow, M. 2014 Annual flood sensitivities to El Niño-Southern oscillation at the global scale. *Hydrology and Earth System Sciences* **18**, 47–66. doi:10.5194/hess-18-47-2014.
- Wilks, D. S. 2006 *Statistical Methods in the Atmospheric Sciences*, second edition. Elsevier Academic Press, Burlington, VT.

First received 28 July 2022; accepted in revised form 27 February 2023. Available online 9 March 2023